Front. For. China 2009, 4(3): 338–343
DOI 10.1007/s11461-009-0050-2

RESEARCH ARTICLE

Wei WANG, Hongjiang ZHANG, Meng LI, Jinhua CHENG, Bo WANG, Weili LU

Infiltration characteristics of water in forest soils in the Simian mountains, Chongqing City, southwestern China

Abstract Spearman rank-correlation analysis and grey relational grade analysis were used to study infiltration characteristics of water in different forest soils in the Simian mountains, Chongqing City. The results indicate that the soil bulk density, contents of coarse sand, and porosity of macropores were significantly correlated with saturated hydraulic conductivity. Porosity of macropores and contents of coarse sand were positively correlated with soil saturated hydraulic conductivity and soil bulk density negatively. Based on the initial infiltration rate, the stable infiltration rate, time required for infiltration to reach a stable state, and cumulative infiltration, all of which are crucial parameters determining soil infiltration capacity, the results of grey relational grade analysis showed that the grey relational grades of the different forest soils were listed from high to low as broad-leaved forest (0.8031) > *Phyllostachys pubescens* forest (0.7869) > mixed conifer-broadleaf forest (0.4454) > coniferous forest (0.4039). Broadleaf forest had the best ability to be infiltrated among the four soils studied. The square roots of the coefficients of determination obtained from fitting the Horton infiltration equation, simulated in our study of forest soils, were higher than 0.950. We conclude that soils of broad-leaved forests were the best suited for infiltration processes of forestry in the Simian mountains.

Keywords Simian mountains, infiltration, Spearman rank-correlation analysis, grey relational grade analysis

1 Introduction

Infiltration of water in soil is an exchange process of precipitation and other forms of water supply between surface runoff and ground water drainage, which has significant effects on the water cycle and soil erosion (Zhang and Wang, 1999). Infiltration characteristics of forest soils are the foundation and a prerequisite for research in runoff mechanisms in forest watershed areas (Philip, 1991). Studies of infiltration parameters under different forest types and evaluation of the ability of forest soils to be infiltrated are both playing an important role in the adjustment mechanism of hydrological watershed processes (Zhou and Hong, 1997; Qi et al., 2006). Soil is composed of water, air, and solid particles of different sizes and shapes. The characteristic of liquid movement is affected by the connectivity of soil pores (Wilson, 1988; Yu et al., 2004). Soil structures determine the diversity and characteristics of physical and hydraulic soil properties. Moreover, soil structures are determined by both the constitution of soil solids and the tactical forms of soil pores (Scoging and Thornes, 1982; Cheng et al., 2007).

Given our experiments and analyses of soil saturated hydraulic conductivity and soil infiltration processes, carried out on four main types of forestland soils in the Simian mountains, the correlation between both physical and hydraulic soil properties and soil infiltrability are discussed and evaluated.

Translated from *Journal of Soil and Water Conservation*, 2008, 22(4): 95–99 [译自: 水土保持学报]

Wei WANG (✉), Hongjiang ZHANG, Meng LI, Jinhua CHENG, Bo WANG, Weili LU
School of Soil and Water Conservation, Key Laboratory of Soil and Water Conservation and Desertification Combating of the Ministry of Education, Beijing Forestry University, Beijing 100083, China
E-mail: vane_bjfu@126.com

2 Materials and methods

2.1 Site description

The field site is the Zhangjiashan in the middle of the Simian mountains located in the southwest of Chongqing City (28°31′14″–28°46′00″N, 106°17′22″–106°30′00″E). The area belongs to the subtropical moist zone of the northern hemisphere. The mean annual temperature is 13.7°C and the frost-free period is 285 days per year. Specifically, the highest monthly mean temperature is 31.5°C in August and the lowest monthly mean temperature is −5.5°C in January. The temperature decreases by 0.58°C for every 100 m increase in elevation. The mean annual rainfall is 1522.3 mm and the highest daily rainfall

is 160.5 mm. The rainy season lasts from May to September and the cumulative rainfall of this period accounts for 62.17% of the mean annual rainfall. Rainfall declines by 43.3 mm for every increase of 100 m in elevation. The mean number of annual cumulative hours of sunlight is 1082.7 h. The number of cumulative hours of sunlight during the growing season (between May and September) accounts for 64% of the mean annual value.

The forest soils are developed from weathered residual material and alluvial deposits, which consist of feldspar, quartz-like sandstone, and siltstone. Yellow-brown earth and yellow earth are the main soil types. The forest soils of our field site are acid and between 10 and 70 cm deep.

The vegetation consists mostly of subtropical evergreen broad-leaved forest. The tree species in the field site are mainly *Cunninghamia lanceolata*, *Pinus massoniana*, *Lithocarpus glaber*, *Schima superba*, *Fokienia hodginsii*, *Cinnamomum camphora*, *Liquidambar formosana*, and *Phyllostachys pubescens*. The bush and grass species are largely *Lespedeza bicolor, Eurya brevistyla*, *Spiraea salicifolia* L., *Carex siderosticta*, and *Setaria palmifolia*.

Sample plots were arranged inside the four main types of forestland, i.e., in a coniferous forest (*C. lanceolata* and *P. massoniana*), a broad-leaved forest (*L. glaber*, *S. superba*, *F. hodginsii, C. camphora*, and *L. formosana*), a mixed conifer-broadleaf forest, and a *P. pubescens* forest. Site conditions of all four sample plots are shown in Table 1.

2.2 Measurement of physical and hydraulic soil properties

In each sample plot, soil profiles (three replications) were dug 60 cm deep. According to the genetic soil horizon, the profile was divided into three layers, with each layer 20 cm thick. Soil samples in each layer were collected for analyzing physical properties such as soil bulk density, porosity, and mechanical composition.

Soil samples in each layer of the plots were measured for saturated hydraulic conductivity by a permeability testing machine (ST-70A, made in China) with a constant head pressure measurement (Shao et al., 2006). The saturated hydraulic conductivity, K_s, was calculated as

$$K_s = \frac{V}{tA} \cdot \frac{L}{H} \quad (1)$$

where H is the constant head of the entrance, V is the flow rate, t is the flow time, L is the length of the earth pillar, and A is the cross-sectional area of the earth pillar.

2.3 Measurement of soil infiltrability

To simulate the field infiltration process, a double ring was used to measure infiltration rates. The double ring consists of an outer loop (25 cm in diameter) and an inner loop (10.5 cm in diameter), with the height of both loops 25 cm. During the experiment, these two loops were driven 10 cm deep into the soil and the water level of both loops was kept at 5 cm. Infiltration measurements were recorded every 5 min.

In the infiltration experiment, the outer environment was stable. The water temperature was kept between 20.8°C and 21.5°C and soil moisture between 15.83% and 18.76%. Therefore, the impact on soil infiltrability generated by soil moisture and water temperature could be ignored.

2.4 Data analysis and statistical methods

Spearman rank-correlation analysis was used to account for the relationships between physical soil properties and saturated hydraulic conductivity (Zhang et al., 2006). The Horton equation was used to simulate the field infiltration process in each forest soil investigated (Hillel, 1998; He et al., 2004). A grey relational grade analysis (Deng, 2005; Wen et al., 2007) was used to evaluate forest soil infiltration capacity.

3 Results and analysis

3.1 Physical and hydraulic soil properties

In soil profiles, saturated hydraulic conductivity is an important parameter in vertical direction for studies of soil water movement; also, it is a crucial index for the evaluation of the ability of soils to be infiltrated. Saturated hydraulic conductivity is closely related to basic physical soil properties, which include soil bulk density, mechanical composition, and porosity.

Table 1 Site condition of forest sample plots

forestland types	site factors			plant condition			litter storage		
	altitude/m	aspect	gradient/°	age/year	canopy density	coverage/%	non-decomposition /(t·hm^{-2})	semi-decomposition /(t·hm^{-2})	decomposition /(t·hm^{-2})
coniferous forest	1183.4	W-N	31°	25	0.60	86	3.94	0.86	197.99
broad-leaved forest	1160.0	E-N	38°	20	0.65	92	2.44	2.57	186.80
mixed conifer-broadleaf forest	1191.5	W-S	15°	20	0.68	90	8.65	10.03	88.41
P. pubescens	1175.3	W-S	19°	25	0.87	63	3.68	7.55	24.14

A correlation analysis was carried out between six soil physical parameters and saturated hydraulic conductivity to indicate the major parameters correlated with saturated hydraulic conductivity. The six parameters in each layer of the forest soil profile were soil bulk density, gravel content (diameter $\geqslant$ 2 mm), coarse sand (0.25 < diameter < 2 mm), fine sand (diameter < 0.25 mm), and porosity of capillary pores and macropores. The physical and hydraulic soil properties of our sample plots are shown in Table 2.

Spearman rank-correlation analysis was used to account for the correlation of the data in Table 2. The results of correlation analysis between soil bulk density, particle contents, porosity, and saturated hydraulic conductivity are shown in Table 3.

In Table 3, it can be seen that soil bulk density and macropores porosity both were significantly correlated with soil saturated hydraulic conductivity at the 0.01 level as well as the contents of coarse sand at the 0.05 level. Furthermore, macropore porosity and the contents of coarse sand were also positively correlated with soil saturated hydraulic conductivity, while soil bulk density was negatively correlated. These results indicate that the impact of physical soil parameters on saturated hydraulic conductivity of forest soil largely came from soil bulk density, from the contents of coarse sand, and from the porosity of macropores. The correlation coefficient of macropores was higher than that of soil bulk density and the contents of coarse sand. Therefore, the number of soil macropores has great effect on soil moisture movement.

Macropores are always considered channels or paths for preferential movement of water and other liquids in the soil. Under gravitational potential, the flux in macropores is higher than that in capillary pores (Zhang and Shangguan, 2006). Saturated hydraulic conductivity of upper layers of the four forest soils studied showed discrepancies. According to our correlation analysis, the differences in forest soil porosity in certain parts of the soil, especially that of macropores, were the main factors contributing to the changes in hydraulic conductivity.

Soil bulk density is a crucial index for describing the condition of soil structures. Lower bulk densities are propitious for developing loose soils, which can improve soil saturated hydraulic conductivity as a result of a decrease in the resistance of water movement in the vertical direction of profiles. The results from our correlation analysis showed that soil bulk density was negatively correlated with saturated hydraulic conductivity. This is similar to the results obtained by Lu et al. (2006).

3.2 Infiltration process

The primary results showed that the Horton equation (Horton, 1940) is precisely applicable for the simulation of infiltration processes in forest soils. The Horton equation is as follows:

$$i = i_c + (i_0 - i_c)e^{-kt} \quad (2)$$

Table 2 Physical and hydraulic soil properties of sample plots

forestland types	depth/cm	bulk density /(g·cm^{-3})	mechanical composition			porosity		saturated hydraulic conductivity/(mm·min^{-1})
			gravel ($\geqslant$2 mm)	coarse sand (2–0.25 mm)	fine sand (< 0.25 mm)	capillary pores /%	macropores /%	
coniferous forest	0–20	1.00	0.16	0.51	0.34	42.56	10.16	4.26
	20–40	1.06	0.22	0.49	0.29	34.63	8.90	3.54
	40–60	1.23	0.04	0.47	0.49	23.41	7.32	2.42
broad-leaved forest	0–20	0.95	0.13	0.49	0.39	37.60	16.72	5.56
	20–40	1.04	0.08	0.54	0.36	35.47	7.16	3.89
	40–60	1.11	0.07	0.36	0.58	41.61	8.07	3.80
mixed conifer-broadleaf forest	0–20	1.01	0.24	0.44	0.32	38.43	7.64	3.52
	20–40	1.25	0.43	0.34	0.22	32.39	4.68	2.51
	40–60	1.45	0.19	0.46	0.36	31.09	5.26	1.95
P. pubescens	0–20	0.88	0.10	0.55	0.35	30.16	15.5	8.66
	20–40	1.03	0.14	0.52	0.34	35.22	5.50	3.15
	40–60	1.10	0.02	0.55	0.43	30.12	12.80	4.21

Table 3 Correlation between saturated hydraulic conductivity and physical soil properties

	bulk density	mechanical composition			porosity	
		gravel	coarse sand	fine sand	capillary pores	macropores
spearman correlation coefficient	−0.790**	−0.245	0.615*	0.147	0.294	0.860**
significance (two-tailed)	0.002	0.443	0.033	0.649	0.354	0.000

Note: * Correlation is significant at 0.05 level (two-tailed). ** Correlation is significant at 0.01 level (two-tailed).

where i is the infiltration rate, t is the infiltration time, i_0 is the initial infiltration rate, i_c is the stable infiltration rate, and k is a constant for infiltration processes.

The data from the double-ring infiltration experiment were simulated by the Horton equation (Eq. 2) on all soil samples. The results of infiltration parameters from simulating the Horton equations by regression analysis are shown in Table 4. The simulated results show that the square roots of the coefficient of determination (R^2) of each forestland infiltration process were all higher than 0.950 and the simulated values are close to the observed values. It is seen that the Horton equation is able to represent the actual field infiltration process. The simulated infiltration processes by the Horton equation are shown in Fig. 1.

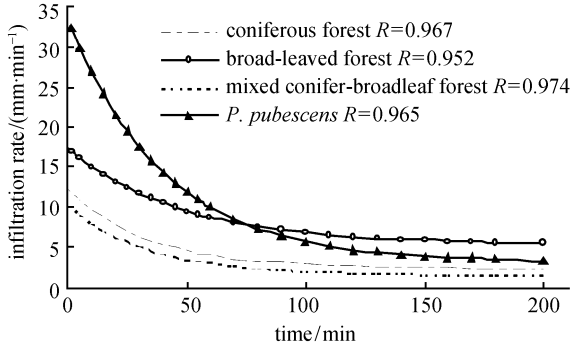

Fig. 1 Infiltration curves for each forestland simulated by Horton equation.

Between our four forestlands investigated, the *P. pubescens* forest had the highest initial infiltration rate at 35.75 mm/min, broad-leaved forests and coniferous forests followed at 17.42 mm/min and 10.75 mm/min, and mixed conifer-broadleaf forest had the lowest initial infiltration rate of only 10.08 mm/min. The initial infiltration rate is largely affected by the surface (depth 0–20 cm) saturated hydraulic conductivity. The surface soil of the *P. pubescens* forest, at 8.66 mm/min, had the highest saturated hydraulic conductivity of these four forestlands followed by the broad-leaved forest at 5.56 mm/min, the coniferous forest at 4.26 mm/min, and the mixed forest with 3.52 mm/min. The saturated hydraulic conductivity of the surface soil coincided perfectly with each initial infiltration rate.

Comparing the stable infiltration rate, it turns out that the broad-leaved forest had the highest rate at 5.35 mm/min, *P. pubescens* and coniferous forest followed at 3.83 mm/min and 2.90 mm/min, and mixed conifer-broadleaf forest had the lowest rate at 1.74 mm/min. The stable infiltration rate was close to the lowest saturated hydraulic conductivity in all four profiles. The saturated hydraulic conductivities of each soil layers had an immediate effect on the infiltration rate. Especially, when the conductivity of the upper layer was less than that of the lower layers, the vertical movement of water was restrained by the resistance generated by the upper soil layer. Residual water had accumulated in this region, and this soil interval was saturated earlier. Therefore, the ability of soil profiles to be infiltrated had declined. Finally, the lowest saturated hydraulic conductivity in each layer was significantly affected by the stable field infiltration rate.

The cumulative infiltration of soils and the time required for infiltration are also able to demonstrate the ability of soils to be infiltrated. According to the results of our double-ring experiments, the interval to reach a stable infiltration state of broad-leaved forest was 80 min, which was longest of the four forestlands. The mixed conifer-broadleaf forest and the *P. pubescens* forest took turns and the time required for infiltration by coniferous forest was shortest at only 50 min. These discrepancies were engendered by soil water-holding capacity, which is determined by soil porosity. The water-holding capacity is the parameter to describe the space for water storage. In the same infiltration process, a higher water-holding capacity requires a longer time for soil to reach saturation level. On the other hand, the interval to reach a stable infiltration state was impacted by the infiltration rate. A higher infiltration rate can cut down the time for a certain soil layer to achieve a saturated condition. Otherwise, the time required for infiltration is related to the presence of rocks and other factors. The cumulative infiltrations until stability was reached in these four forestlands were as follows: *P. pubescens* forest (951 mm), broad-leaved forest

Table 4 Measured and simulated infiltration parameters of each forestland

forestland types	measured				simulated			
	initial infiltration rate /(mm·min^{-1})	stable infiltration rate /(mm·min^{-1})	infiltration duration/min	cumulative infiltration/mm	initial infiltration rate /(mm·min^{-1})	stable infiltration rate /(mm·min^{-1})	infiltration duration/min	cumulative infiltration/mm
coniferous forest	10.75	2.90	50	334	11.48	2.78	60	372
broad-leaved forest	17.42	5.35	80	866	16.57	5.53	70	794
mixed conifer-broadleaf forest	10.08	1.74	70	342	9.23	1.87	80	381
P. pubescens	35.75	3.83	60	951	31.11	3.97	70	1020

(866 mm), mixed broadleaf-conifer forest (342 mm), and coniferous forest (334 mm).

3.3 Evaluation of soil infiltration capacity

The process of soil water infiltration can be divided into three stages: an initial infiltration stage, a transition stage, and a stable infiltration stage. These three rates and the cumulative infiltration are four important parameters reflecting the infiltration capacity of forest soils investigated. These parameters can also describe the characteristics of the entire infiltration process. In our study, the initial infiltration rate, the stable infiltration rate. and the time required until infiltration reached its state of stability and the cumulative infiltration at its state of stability were selected as the indices for evaluating, by a grey relational grading method, the ability of forest soils to be infiltrated.

The grey relational grade analysis is an effective analytical method to analyze the correlation between small samples. This method analyzes and confirms the effect between factors or contribution of factors to the main action (Deng, 2005).

Before a grey relational grade analysis could be applied, the four factors chosen to reflect the infiltration capacity of the soils had to be transformed in order to obtain standardized data. The aim of standardization is to eliminate the effect of different dimensions. The maximum of each parameter was its optimum value, so that the maximum in every group of data was selected as the criterion-referenced value, where each group of data was divided by the maximum of the particular group in order to obtain new data series. The parameters of the standardized data series for infiltration capacity evaluation are shown in Table 5.

According to the grey relational grade analysis with standardized data, the grey relational coefficients and grades of each forestland are shown in Table 6. A grey relational coefficient of an evaluation index indicates the correlation between the index and its optimum value. It means that the closer the grey relational coefficient is to 1.000, the better the ability of the index. The grey relational grade is the arithmetic mean of grey relational coefficients, which denotes the infiltration capacity of each forest soil.

According to the grey relational grades, the ability of these four soils to be infiltrated is listed in order from high to low as broad-leaved forest (0.8031) > *P. pubescens* forest (0.7869) > mixed conifer-broadleaf forest (0.4454) > coniferous forest (0.4039). The broadleaf forest had the highest grey relational coefficients between infiltration rates and the time required to reach saturation of these four forest soils and it can drain the surface water quickly. The soil water-holding capacity of the broad-leaved is excellent. Broadleaf forests can effectively support more space for water storage and reduce surface runoff; therefore, the soil erosion generated by runoff is decreased. Finally, it should be mentioned that the broad-leaved forest had the optimum ability, of the four forest soils investigated, to be infiltrated.

4 Conclusions

The results of Spearman rank-correlation analysis between soil bulk density, mechanical composition, porosity, and saturated hydraulic conductivity showed that the soil bulk density, contents of coarse sand, and porosity of macropores were significantly correlated with saturated hydraulic conductivity. Macropore porosity and the contents of coarse sand were both positively correlated with soil saturated hydraulic conductivity. Soil bulk density was negatively correlated with soil saturated hydraulic conductivity.

The square roots of the coefficients of determination simulated by the Horton infiltration equation in each of the

Table 5 Standardized data of water infiltration parameters on each forestland

forestland types	initial infiltration rate	stable infiltration rate	infiltration time	cumulative infiltration
coniferous forest	0.2986	0.5273	0.6250	0.3512
broad-leaved forest	0.4872	1.0000	1.0000	0.9106
mixed conifer-broadleaf forest	0.2820	0.3258	0.8750	0.3596
P. pubescens	1.0000	0.7159	0.7500	1.0000

Table 6 Grey relational coefficients and grades of water infiltration characteristic of different forest soils

forestland types	grey relational coefficient				grey relational grade
	initial infiltration rate	stable infiltration rate	infiltration time	cumulative infiltration	
coniferous forest	0.3386	0.4316	0.4891	0.3562	0.4039
broad-leaved forest	0.4118	1.0000	1.0000	0.8007	0.8031
mixed conifer-broadleaf forest	0.3333	0.3475	0.7417	0.3592	0.4454
P. pubescens	1.0000	0.5582	0.5895	1.0000	0.7869

four forest sample plots investigated were higher than 0.950 and we conclude therefore that the equation has a good applicability in forest soil infiltration processes in the Simian mountains.

Based on the initial infiltration rate, the stable infiltration rate, the time required for infiltration to reach a stable state, and the cumulative infiltration, which were the important parameters determining soil infiltration characteristics, the results from our grey relational grade analysis showed that the grey relational grades of the different forest soils are listed, from high to low, as broad-leaved forest (0.8031) > *P. pubescens* forest (0.7869) > mixed conifer-broadleaf forest (0.4454) > coniferous forest (0.4039). The broadleaf forest had the best infiltration capacity among the four forest soils investigated.

Acknowledgements The study was jointly supported by the National Natural Science Foundation of China (No. 40771042), the Introduction of Advanced International Forestry Science and Technology Plan of the State Forestry Administration China (No. 2006-4-26) and the National Forestry Science and Technology Support Program of China (No. 2006BAD03A1304).

References

Cheng J H, Zhang H J, Zhang Y Y (2007). Affecting factors of preferential flow in the forest of the Three Gorges area, Yangtze River. Front For China, 2(4): 436–442

Deng J L (2005). The Primary Methods of Grey System Theory (2nd ed.). Wuhan: Huazhong University of Science and Technology Press, 74–85

He F, Zhang H J, Shi Y H (2004). Pipe flow and infiltration on granite slope in Three Gorges area of the Yangtze River. Bull Soil Water Conserv, 24(6): 10–13, 44 (in Chinese)

Hillel D (1998). Environmental Soil Physics. New York: Academic Press, 391–393

Lu D Q, Shao M A, Liu C P (2006). Effect of bulk density on soil saturated water movement parameters. J Soil Water Conserv, 20(3): 154–157 (in Chinese)

Philip J R (1991). Hill slope infiltration divergent and convergent slopes. Water Resour Res, 27: 1035–1040

Qi S L, Zhang H J, He F (2006). Field experiments and finding on the relationship of infiltration and runoff with rainfall on forest granitic slope at Three Gorges of Yangtze River. J Engin Geol, 14 (3): 365–369 (in Chinese)

Scoging H M, Thornes J B (1982). Infiltration Characteristics in a Semiarid Environment. Wallingford: IAHS Publication, 159–168

Shao M A, Wang Q J, Huang M B (2006). Soil Physics. Beijing: Higher Education Press, 84–85 (in Chinese)

Wen X S, He B H, Zhang H J (2007). Application of grey correlation analysis in the evaluation of different agroforestry planting patterns in the Three Gorges reservoir area. J Southwest Agric Univ (Nat Sci Ed), 29(7): 111–115(in Chinese)

Wilson G V, Luxmoore R J (1988). Infiltration, macroporosity and mesoporosity distribution on two forested watersheds. Soil Sci Soc Am J, 52: 329–335

Yu X X, Zhao Y T, Zhang Z Q (2004). Characteristics of soil water infiltration in subalpine dark coniferous ecosystem of upper reaches of Yangtze River. Chin J Appl Ecol, 14(1): 15–19 (in Chinese)

Zhang G P, Zhang F, Ru W M (2006). Interspecific correlations among dominant populations of ligneous species in Mianshan Mountain of Shanxi. Chin J Ecol, 25(3): 295–298 (in Chinese)

Zhang H J, Wang L X (1999). Soil Loss Characteristics in the Slope in the Three Gorges and Its Dynamic Modeling. Beijing: Chinese Forestry Publishing House, 34–36 (in Chinese)

Zhang X B, Shangguan Z P (2006). Effect of human-induced disturbance on physical properties of soil in artificial *Pinus tabulaeformis* Carr. forests of the Loess Plateau. Acta Ecol Sin, 26(11): 3685–3695 (in Chinese).

Zhou Z F, Hong L X (1997). Studies on infiltration and infiltration simulation of soil water in different woodlands. Sci Silv Sin, 33(1): 9–16 (in Chinese)